

N63-22946

NASA TECHNICAL NOTE



NASA TN D-2029

NASA TN D-2029

**WATER-FILM COOLING OF AN 80°
TOTAL-ANGLE CONE AT A MACH
NUMBER OF 2 FOR AIRSTREAM TOTAL
TEMPERATURES UP TO $3,000^\circ$ R**

*by Howard S. Carter
Langley Research Center
Langley Station, Hampton, Va.*

TECHNICAL NOTE D-2029

WATER-FILM COOLING OF AN 80° TOTAL-ANGLE CONE
AT A MACH NUMBER OF 2 FOR AIRSTREAM TOTAL
TEMPERATURES UP TO $3,000^{\circ}$ R

By Howard S. Carter

Langley Research Center
Langley Station, Hampton, Va.

NATIONAL AERONAUTICS AND SPACE ADMINISTRATION

TECHNICAL NOTE D-2029

WATER-FILM COOLING OF AN 80° TOTAL-ANGLE CONE AT

A MACH NUMBER OF 2 FOR AIRSTREAM TOTAL

TEMPERATURES UP TO $3,000^\circ \text{ R}^1$

By Howard S. Carter

SUMMARY

Film-cooling tests, with water as the coolant, were made on an 80° total-angle cone in a Mach number 2 free jet at sea-level pressure. The tests were made at free-stream total temperatures from $1,500^\circ$ to $3,000^\circ \text{ R}$ and at free-stream Reynolds numbers per foot from 8×10^6 to 3×10^6 .

The tests showed that the downstream end of the model became very hot if the coolant rate was too small to cover the complete model with a water film. This water film was fairly symmetrical when the model was at zero angle of attack but was very asymmetrical when the model was at an angle of attack of 5° . A comparison with results of a previous transpiration-cooling test showed that, with water as the coolant, transpiration cooling was at least 2.5 times as efficient as the film cooling of the present tests.

INTRODUCTION

The survival of a long-range ballistic missile during atmospheric reentry depends to a great extent upon alleviating the heating load to the nose region. (See refs. 1, 2, and 3.) It has been determined from previous work that for large weight-drag ratios the problem cannot be solved by geometric considerations alone, such as blunting the nose or redistributing the material in the nose to improve the absorption of the incoming heat. Hence, many different cooling schemes have been suggested for keeping the nose of the reentry missile at a temperature that present materials can withstand. At present, however, the data available on the different cooling schemes are insufficient for direct

¹Supersedes NASA Memorandum 12-27-58L by Howard S. Carter, 1959.

application to a given missile nose without some preliminary tests in which the actual proposed missile-nose shape and cooling scheme are used.

A program was initiated by the Pilotless Aircraft Research Division of the Langley Aeronautical Laboratory to determine the feasibility of using a film-cooling scheme on a proposed nose shape of a current missile. The proposed nose shape was an 80° total-angle cone and the coolant was distilled water ejected at the apex of the cone. The local airstream swept this water back over the surface of the cone in the form of a water film.

The parameters which varied in this present investigation were free-stream total temperature, angle of attack, coolant flow rate, and geometry of coolant ejection nozzle. The tests were made in the ethylene-heated high-temperature jet of the Langley Pilotless Aircraft Research Station at Wallops Island, Va. All tests were made in this 12-inch-diameter jet at sea-level pressure for a Mach number of 2.03. The values of free-stream total temperature for the tests were approximately $1,500^\circ$, $2,000^\circ$, $2,500^\circ$, and $3,000^\circ$ R. Axial-type coolant nozzles of three different diameters and one umbrella-type coolant nozzle were used in the tests. The free-stream Reynolds number per foot varied during the testing program from 3×10^6 to 8×10^6 .

SYMBOLS

A	area, sq ft
α	angle of attack, deg
h	aerodynamic heat-transfer coefficient, Btu/(sec)(sq ft)($^\circ$ R)
p	pressure, lb/sq ft
q_l	local heat-transfer rate, Btu/(sec)(sq ft)
Q_A	actual no-coolant heat load, Btu/sec
Q_T	theoretical no-coolant heat load, Btu/sec
r	radius, ft
ρ	density of gas flow, lb/cu ft
S	distance along cone surface meridian from apex, ft

T	temperature, °R
V	velocity of gas flow, ft/sec
W	weight of coolant per unit area of model, lb/sec per sq ft of model wetted area
M	Mach number

Subscripts:

aw	adiabatic wall
c	coolant
∞	free stream
l	local
t	total
w	wall

APPARATUS

Model

The model, shown in figure 1, was an 80° total-angle cone with a base diameter of 5.75 inches which was fabricated from type 347 stainless steel. The wall thickness of the cone was 0.050 inch. A tube was installed along the axis of the cone, terminating at the apex where coolant flow nozzles of various size and geometry could be inserted.

Drawings of the coolant nozzles are shown in figure 2. Three of the nozzles had straight through holes with inside diameters of 0.050, 0.150, and 0.200 inch. An umbrella nozzle designed to direct the flow tangentially over the body was also used. All nozzles were made of stainless steel and had external screw threads for mounting in the nose of the cone.

The locations of the thermocouples and pressure orifices are shown in figure 1. There were 20 chromel-alumel thermocouples installed on the inner surface of the cone along the two meridians in the pitch plane. Ten thermocouples were also installed on the inner surface at station 1.70 so that a thermocouple was located every 30° around the body. The water

temperature was measured with a copper-constantan thermocouple located in the coolant flow pipe at approximately the location shown on the drawing.

Seven pressure orifices were installed along the two meridians at right angles to the thermocouple meridians. One additional orifice was located on one of the thermocouple meridians. The locations of these eight orifices are shown in figure 1. All pressure tubes were soldered to the stainless-steel model with a silver solder that has a melting point of $1,175^{\circ}$ F.

Test Facility

The tests were made in a 12-inch-diameter ethylene-heated high-temperature jet of the Langley Pilotless Aircraft Research Station at Wallops Island, Va. This jet is a blowdown-type system consisting of storage spheres, a preheater, combustion chamber, and test nozzles. Air is kept in the storage spheres at a pressure of about 200 pounds per square inch and a dewpoint temperature of about -40° F. During operation, air from the spheres is preheated to approximately 900° R and passed through ducts into a combustion chamber where ethylene is injected into the airstream. Ignition is obtained by firing a small solid-propellant rocket into the ethylene-air mixture. The products of the resulting combustion are passed through the 12-inch-diameter nozzle and exhausted at ambient sea-level pressure to obtain shock-free flow at a Mach number of 2.03. The temperature of the exhaust gas is varied by changing the ethylene-air ratio, and the static pressure of the exhaust gas is regulated with a valve upstream of the combustion chamber. The physical characteristics of this jet are discussed more fully in reference 4.

Figure 3 shows the model, with the umbrella nozzle, mounted in the jet. The upstream tip of the model was approximately 1.5 inches downstream of the exit plane of the jet nozzle, and the axes of the model and this nozzle coincided. The model was mounted on an elbow-shaped stand which encased all the thermocouple wires and pressure tubes to protect them from the high-temperature free stream. This elbow-shaped stand was mounted on a hydraulically operated, pivoted model support which provided for swinging the model into the test section after equilibrium conditions were reached. At the completion of each test the model was swung out of the jet before shutdown. Thus, the model was not subjected to the transient flow conditions which occur during the starting and shutdown of the jet.

TESTS

All tests were made in the free jet at $M = 2.03$ with approximately sea-level static pressure conditions at the jet exit and at nominal free-stream total temperatures of $1,500^{\circ}$, $2,000^{\circ}$, $2,500^{\circ}$, and $3,000^{\circ}$ R. The basic data for all tests are given in table I. The variation of temperature during each test was not more than $\pm 50^{\circ}$ R, which was considered acceptable. The free-stream Reynolds number per foot varied from 8×10^6 at a free-stream temperature of about $1,500^{\circ}$ R to 3×10^6 at a free-stream temperature of about $3,000^{\circ}$ R.

At approximately $1,500^{\circ}$ R, a test was made with each coolant flow nozzle. The clearance between the umbrella nozzle and the model surface was 0.0025 inch. No significant differences in cooling were noted between any of these tests at $1,500^{\circ}$ R, regardless of coolant-nozzle geometry. Hence, at $2,000^{\circ}$ R, only the 0.150-inch-diameter axial nozzle and the umbrella nozzle (0.0025-inch clearance) were used. Also, at $2,000^{\circ}$ R no significant differences in cooling were noted between the two types of nozzles. Hence, at $2,500^{\circ}$ R and at $3,000^{\circ}$ R only the 0.150-inch-diameter axial nozzle was used. To provide a basis for evaluating the effectiveness of these film-cooling tests, a test was performed without coolant at an arbitrarily chosen temperature of $1,500^{\circ}$ R. Also, to determine the effect of angle of attack on the flow symmetry, a test was made at $1,500^{\circ}$ R with each of the two types of coolant ejection nozzles at an angle of attack of 5° .

At the beginning of each test, the model was held out of the jet until the free-stream flow became steady. Then the coolant flow was started at a high rate and the model was swung into the jet. It took approximately 1 second for the model to reach the center line of the jet. When the model reached the center line, a microswitch on the arm of the injector stand made contact and the resulting signal was indicated on the recorder. The test then continued at sea-level free-stream pressure for approximately 40 seconds. During this time the coolant flow rate was reduced in steps until the downstream end of the model got hot. Then the coolant flow rate was increased in steps until approximately the original flow rate was obtained. No attempt was made to obtain identical decreasing and increasing stepwise flow rates.

RESULTS AND DISCUSSION

Pressure Distributions

A typical pressure distribution for each of the two different types of coolant flow nozzles is shown in figure 4. In these plots the local

surface pressure on the cone is expressed as a fraction of the free-stream stagnation pressure and plotted against model station. The data in this figure are for tests B-1807 (using a 0.150-inch-diameter axial coolant nozzle) and for B-1808 (using the umbrella coolant nozzle). The two identical symbols at each station represent the pressures for the two orifices at each station. Since there were no significant differences in the pressures on opposite meridians of the model, the angle of attack was apparently very close to zero.

The pressure distributions in figure 4 agree closely with those for all the other tests at zero angle of attack. The pressure distributions were apparently unaffected by changes in the diameter of axial coolant nozzles, in free-stream total temperature, and in coolant flow rate. Different types of nozzles, however, caused differences in the pressure distributions. The pressures near the tip of the cone were considerably less with the umbrella nozzle than with the axial flow nozzles. The tip geometry of the model was different for these two types of coolant nozzles. Apparently the local airstream on the forward part of the model expanded more when the umbrella nozzle was used, causing the low-pressure region shown in figure 4.

The pressure distribution predicted by cone theory (assuming a sharp tip) is also shown in figure 4. The pressures from both tests approach the theoretical pressure at the downstream end. Evidently the blunt tip of each nozzle forced the cone shock to be detached and hence caused the pressures over the whole model surface to be less than the theoretical pressures.

Temperature Distributions

Shown in figure 5 is the temperature distribution for a series of coolant rates for a typical test (B-1807). The temperatures are presented in the form of the parameter $T_w - T_c / T_{aw} - T_c$ where T_w is the equilibrium temperature of the cooled wall, T_{aw} is the theoretical equilibrium temperature of the uncooled wall, and T_c is the original temperature of the water.

The data for each test were obtained by decreasing the coolant flow rate in steps until the model became hot on the downstream end and then increasing it in steps to approximately the original rate. The method of plotting used in figure 5 depicts the approximate temperature distribution on the model surface for each coolant flow rate and assisted in the fairing of the data toward a family of curves.

The model was constructed to allow temperatures to be obtained on opposite meridians. In addition, several temperature measurements were

to be obtained at the 1.70-inch station on other meridians. In general, all the temperatures at the 1.70-inch station were in good agreement. Hence, to simplify the plot, only the temperatures on the two primary temperature-measuring meridians are plotted in figure 5. Some of the thermocouples were inoperative during the tests, and thus a complete temperature distribution on each of the two meridians could not be obtained. The temperatures that could be plotted are shown in the figure. Double symbols for a given station represent the temperatures on the two opposite meridians of the model. The agreement for most stations was good.

Figure 5 indicates that the water film for the four highest coolant flow rates extended completely to the measuring station farthest downstream; however, for the four lower coolant flow rates, the water film did not extend that far. For these lower coolant flow rates, a thermocouple on one side of the model would sometimes be covered with a water film while that on the opposite side at the same station would not. This fact indicated an asymmetry which appeared from the temperature distributions to be small in area. This slight asymmetry of the water film helped in some cases to locate more closely the downstream extent of the water film. The basic temperature data are given in table I.

Temperature and Coolant-Rate Parameters

A composite plot of temperature parameter against coolant-rate parameter is shown in figure 6 for all tests at zero angle of attack. The temperature parameter in this figure is for the thermocouple station farthest downstream, where the maximum temperatures always occurred. A similar plot of this type could be made for any other station on the model; however, the point of maximum temperature will be of greatest interest to the designer of a cooling system.

As the free-stream total temperature was increased the data, as shown in figure 6, became more sparse. This made the fairing of the higher temperature data somewhat in doubt. However, since the fairing of the 1,500° R data was fairly well established, the data at other temperatures were faired with a similar curve. At a free-stream total temperature of 3,000° R, no recorded data were obtained for coolant flow rates low enough to cause the model to become hotter than the boiling point. For this test, the break in the temperature curve was made at the lowest flow rate. A visual indicator used for monitoring revealed, during this 3,000° R test, that the downstream thermocouple station (thermocouple 1) was becoming hot at this low flow rate. The operator did not reduce the flow rate further for fear that the model would become hot enough to melt out the silver solder holding the pressure tubes in place. Therefore, from visual data that are not presented

in this figure, it is believed that the fairing of the data for $3,000^{\circ}\text{R}$ is approximately correct.

As indicated on figure 6, four different coolant nozzles were used in the tests at $1,500^{\circ}\text{R}$ and two at $2,000^{\circ}\text{R}$. There were no significant differences in the results due to differences in the coolant nozzles.

The dashed curve which represents the locus of boiling points on the figure was calculated for each of the free-stream total temperatures. This was done by calculating the value of $T_w - T_c/T_{aw} - T_c$ for boiling at each free-stream total temperature and then fairing the dashed curve so that it would pass through the solid $T_{t,\infty}$ curves at the respective boiling point values. For values of the flow parameter between 0 and 0.0014, the curve was faired from a knowledge of the two end points and the approximate point at $1,000^{\circ}\text{R}$. The value of $T_w - T_c/T_{aw} - T_c$ for boiling was calculated for $1,000^{\circ}\text{R}$ as for the other $T_{t,\infty}$. At a $T_{t,\infty}$ value of $1,000^{\circ}\text{R}$, the value of flow-rate parameter was obtained by a cross fairing of $T_{t,\infty}$ against flow-rate parameter as shown in figure 7.

Figure 7 presents the minimum flow rates necessary to maintain the water film to the thermocouple station farthest downstream at different free-stream total temperatures. For free-stream temperatures above $1,500^{\circ}\text{R}$, this curve apparently is a straight-line function of the free-stream total temperature. Below $1,500^{\circ}\text{R}$, the curve was faired to the calculated end point at a flow-rate parameter of zero. The minimum flow rate necessary to cool the entire model at $T_{t,\infty} = 1,000^{\circ}\text{R}$ is seen from this curve to be 0.0003. This is the value of flow-rate parameter at which the boiling point was plotted in figure 6 for $T_{t,\infty} = 1,000^{\circ}\text{R}$.

As mentioned previously, the data in figure 6 are all for the thermocouple station farthest downstream. When the water rate is just sufficient to cover the model with a film back to this point, the temperature parameter at this station is seen to correlate very well with the boiling-point curve. The data of reference 5 for the station at the downstream end of the water film are shown in figure 6 by a solid symbol which also correlates with this boiling-point curve.

If the data are correlated on the basis of average surface temperature, different results will be obtained. At low heating rates such as existed in the tests of reference 5 ($T_{t,\infty} = 1,000^{\circ}\text{R}$), the average temperature correlates very closely with the saturated vapor temperature. At high heating rates such as existed in the present tests at $T_{t,\infty} = 3,000^{\circ}\text{R}$, the average temperature correlates better with the boiling temperature.

Efficiency of Film Cooling

The primary purpose of making these film-cooling tests was to obtain the data shown in figure 6. However, since the present method of cooling is not the only one that is being considered for possible use in cooling reentry models, some of the data are also presented in a form that shows the effectiveness or efficiency of the film-cooling method. Also, in this form the data from other cooling methods can be compared with the film-cooling method used in the present tests.

Figure 8 presents the data in the form of an efficiency factor Q_A/Q_T plotted against coolant flow-rate parameter $W/\rho_l V_l$. As used in this report, Q_A is the actual no-coolant heat load that would have existed on the model at the wall temperature of the cooling test. It was obtained by integrating the local heat loads over the complete model surface. The local heat loads were calculated for each station from the equation

$$q_l = h_l (T_{aw,l} - T_{w,l})$$

Then the actual no-coolant total heat load was obtained from the following integration

$$Q_A = \int_A q_l \, dA = 2\pi \int_S q_l r_l \, dS$$

This value of Q_A may not be the actual value of heat that is being absorbed by the water film, since the heat-transfer coefficient and equilibrium wall temperature may have varied considerably from their values on the dry wall. Reference 6 shows how the presence of a water film varies the heat-transfer coefficient, and reference 7 shows how the presence of a coolant varies the equilibrium wall temperature. This value of Q_A is a good reference number, however, that can be readily calculated for most model shapes for a given wall temperature.

As used in this report, Q_T is the theoretical no-coolant heat load that could have existed on the model at the wall temperature of the cooling test, based on the assumption that the full cooling capacity of the water was used. It was obtained by calculating the total heat necessary to raise the cooling water from its entering enthalpy to its final enthalpy. It may be shown in equation form as

$$Q_T = WA(\text{Coolant final enthalpy} - \text{Coolant entering enthalpy})$$

The coolant final enthalpy was always based on the average wall temperature of the model or on the boiling temperature of water on the model, whichever was greater. Always included in Q_T was the heat of vaporization.

Figure 8 shows that at each value of $T_{t,\infty}$ the efficiency increased as the coolant flow rate decreased. For some reason the curves all seemed to tend toward $Q_A/Q_T = 0.40$. This would seem to indicate that this method of film cooling is limited in efficiency to 40 percent.

The minimum value of the flow rate parameter corresponding to complete coverage of the model with a water film was determined for each value of $T_{t,\infty}$ in the present tests and in reference 5. The locus of these points in figure 8 is the straight line at $Q_A/Q_T = 0.26$. Hence, the film cooling used in these tests is approximately 26 percent efficient if the minimum value of coolant flow rate is used to maintain a water film on the complete model. If more than this flow rate is used the efficiency decreases, and if less than this flow rate is used the efficiency increases. A disadvantage of decreasing the flow rate, however, is that the downstream end of the model becomes hot.

Also shown in figure 8 are the data from reference 8 which present the results of transpiration-cooling tests on an 8° total-angle cone at $T_{t,\infty} = 1,000^\circ \text{ R}$. At the highest three flow rates of these transpiration tests the model temperature was maintained at approximately 125° to 140° F . At the lowest flow rate the flow was unsymmetrical as a result of gravity effects and part of the model became hot. From the data as presented in reference 8, it appears that this lowest flow rate would also have cooled the model below saturated steam temperature if the gravity effects had not existed. Hence, the straight line in figure 8 at $Q_A/Q_T = 0.65$ is only approximate and perhaps should be at an even higher value. This $Q_A/Q_T = 0.65$ is the approximate level of efficiency for minimum flow rates necessary to keep the complete model surface below saturated steam temperature. It appears from figure 8 that the transpiration-cooling method of reference 8 was at least 2.5 times as efficient as the film cooling of the present tests.

Effect of Angle of Attack

Included in the program were two tests at $\alpha = 5^\circ$ to determine the effect of angle of attack on the symmetry of the water film. The basic

data from these two tests are given in table I. These tests were not originally intended to be included in the program. Hence, the model was not oriented in the jet to give the best data; that is, the main thermocouple meridians were not on the leeward and windward sides of the model but were 90° from these positions. However, motion pictures of the tests and sediment rings on the model indicated that the water film on the model surface was very asymmetrical at $\alpha = 5^\circ$.

Two sketches (fig. 9) depict approximately this water-film asymmetry at $\alpha = 5^\circ$ for each type of nozzle. It was thought that the umbrella-type nozzle would be less affected by angle of attack than the axial-type nozzle. However, the motion pictures and sediment rings did not show any significant difference between the two types of nozzles. Apparently this water film starts fairly symmetrically at the tip of the cone but, as a result of boundary-layer cross flow or pressure differences, the coolant is forced from the windward side to the leeward side.

SUMMARY OF RESULTS

Film-cooling tests, with water as the coolant, were made on an 80° total-angle cone in a free jet at sea-level pressure. The Mach number of the tests was 2.03 and the free-stream total temperatures were approximately $1,500^\circ$, $2,000^\circ$, $2,500^\circ$, and $3,000^\circ$ R. The following results were obtained:

1. As the coolant rate was progressively reduced below the minimum required to keep a water film on the complete model, the temperature at the downstream end of the model became progressively higher.
2. There were no significant differences between the cooling results achieved with the axial nozzle and with the umbrella nozzle.
3. For the minimum coolant rates necessary to cover the complete model with a water film, the efficiency for all tests was approximately 26 percent, based on the total cooling capacity of the water.
4. When water is used as the coolant, transpiration cooling is at least 2.5 times as efficient as the film cooling of the present tests.
5. The water film on the model surface was fairly symmetrical for all tests at $\alpha = 0^\circ$ but was very asymmetrical for all tests at $\alpha = 5^\circ$.

Langley Research Center,
National Aeronautics and Space Administration,
Langley Field, Va., July 17, 1958.

REFERENCES

1. Allen, H. Julian, and Eggers, A. J., Jr.: A Study of the Motion and Aerodynamic Heating of Ballistic Missiles Entering the Earth's Atmosphere at High Supersonic Speeds. NACA Rep. 1381, 1958. (Supersedes NACA TN 4047.)
2. Carter, Howard S., and Bressette, Walter E.: Heat-Transfer and Pressure Distribution on Six Blunt Noses at a Mach Number of 2. NACA RM L57C18, 1957.
3. Purser, Paul E., and Hopko, Russell N.: Exploratory Materials and Missile-Nose-Shape Tests in a 4,000° F Supersonic Air Jet. NACA RM L56J09, 1956.
4. English, Roland D., Spinak, Abraham, and Helton, Eldred H.: Physical Characteristics and Test Conditions of an Ethylene-Heated High-Temperature Jet. NACA TN 4182, 1958.
5. O'Sullivan, William J., Chauvin, Leo T., and Rumsey, Charles B.: Exploratory Investigation of Transpiration Cooling to Alleviate Aerodynamic Heating on an 8° Cone in a Free Jet at a Mach Number of 2.05. NACA RM L53H06, 1953.
6. Kinney, George R., Abramson, Andrew E., and Sloop, John L.: Internal-Liquid-Film-Cooling Experiments With Air-Stream Temperatures to 2,000° F in 2- and 4-Inch-Diameter Horizontal Tubes. NACA Rep. 1087, 1952. (Supersedes NACA RM E50F19 by Kinney and Sloop, NACA RM E51C13 by Kinney and Abramson, and NACA RM E52B20 by Kinney.)
7. Rubesin, Morris W., Pappas, Constantine C., and Okuno, Arthur F.: The Effect of Fluid Injection on the Compressible Turbulent Boundary Layer - Preliminary Tests on Transpiration Cooling of a Flat Plate at $M = 2.7$ With Air As the Injected Gas. NACA RM A55I19, 1955.
8. Chauvin, Leo T., and Carter, Howard S.: Exploratory Tests of Transpiration Cooling on a Porous 8° Cone at $M = 2.05$ Using Nitrogen Gas, Helium Gas, and Water as the Coolants. NACA RM L55C29, 1955.

TABLE I.- BASIC DATA

(a) Test B-1805

Coolant nozzle

Type	Axial
Diameter, in.	0.200
Temperature of coolant, °R	515
Total temperature of free stream, °R	1,500
Static pressure of free stream, lb/sq in. abs	14.40
Total pressure of free stream, lb/sq in. abs	120.4
α , deg	0
Model surface pressure, lb/sq in. abs, at -	
Orifice 1	54.6
Orifice 2	49.3
Orifice 3	50.3
Orifice 4	49.8
Orifice 5	51.2
Orifice 6	50.9
Orifice 7	55.3
Orifice 8	57.4

Thermocouple	Temperature on cooled wall, °R, for coolant flow rate, lb/sec, of -				
	0.0875	0.0670	0.0500	0.0347	0.0194
1	691	690	708	-----	1,330
2	710	675	710	1,340	1,300
3	---	---	---	-----	-----
4	683	672	672	790	1,175
5	679	672	672	740	740
6	665	660	658	684	680
7	655	655	655	676	668
8	644	650	650	677	666
9	617	630	635	668	657
10	529	585	593	636	637
11	573	570	577	589	588
12	636	630	631	668	672
13	648	655	648	676	692
14	682	675	663	687	763
15	678	669	667	683	756
16	680	665	664	691	1,215
17	732	660	655	726	1,208
18	707	663	663	772	990
19	722	663	686	1,063	1,315
20	---	---	---	-----	-----
21	678	669	670	763	800
22	675	660	658	676	726
23	---	665	655	675	-----
24	669	667	667	677	780
25	668	665	665	675	750
26	668	665	665	738	860
27	669	667	669	681	698
28	665	665	667	686	686
29	---	667	669	697	-----
30	681	660	660	686	693

TABLE I.- BASIC DATA - Continued

(b) Test B-1807

Coolant nozzle	
Type	Axial
Diameter, in.	0.050
Temperature of coolant, °R	515
Total temperature of free stream, °R	1,460
Static pressure of free stream, lb/sq in. abs	14.80
Total pressure of free stream, lb/sq in. abs	120.4
α , deg	0
Model surface pressure, lb/sq in. abs, at -	
Orifice 1	54.3
Orifice 2	51.4
Orifice 3	51.1
Orifice 4	50.8
Orifice 5	53.1
Orifice 6	52.6
Orifice 7	55.0
Orifice 8	57.5

Thermocouple	Temperature on cooled wall, °R, for coolant flow rate, lb/sec, of -							
	0.0695	0.0611	0.0514	0.0447	0.0410	0.0319	0.0285	0.0181
1	713	687	731	780	1,020	1,138	1,210	1,210
2	684	683	705	737	806	1,073	1,176	1,166
3	---	---	---	---	---	---	---	---
4	668	668	673	679	702	690	724	923
5	664	664	668	668	668	679	685	702
6	654	654	654	699	654	660	660	670
7	656	667	661	656	667	661	661	639
8	650	662	641	656	---	661	650	662
9	636	691	685	642	658	653	653	659
10	---	---	---	---	---	---	---	---
11	585	573	568	573	573	585	577	584
12	642	652	647	642	652	656	658	658
13	656	661	661	656	667	661	661	667
14	688	703	651	688	703	696	696	742
15	667	672	667	667	679	684	686	751
16	665	661	665	665	676	700	734	1,049
17	---	---	---	---	---	---	---	---
18	681	660	687	725	720	1,084	1,185	1,196
19	712	686	708	744	744	1,121	1,220	1,213
20	---	---	---	---	---	---	---	---
21	667	689	696	672	718	689	778	785
22	654	660	660	654	666	660	700	711
23	---	---	---	---	---	---	---	---
24	663	656	663	663	656	671	671	708
25	660	660	660	660	660	660	665	684
26	660	660	660	666	670	707	686	---
27	662	662	662	662	662	667	671	688
28	658	657	663	658	663	663	672	688
29	---	---	---	---	---	---	---	---
30	661	667	667	661	667	671	671	667

TABLE I.- BASIC DATA - Continued

(c) Test B-1808

Coolant nozzle

Type	Umbrella
Clearance, in.	0.0025
Temperature of coolant, °R	510
Total temperature of free stream, °R	1,460
Static pressure of free stream, lb/sq in. abs	14.80
Total pressure of free stream, lb/sq in. abs	120.4
α , deg	0
Model surface pressure, lb/sq in. abs, at -	
Orifice 1	56.4
Orifice 2	52.4
Orifice 3	39.5
Orifice 4	40.1
Orifice 5	54.3
Orifice 6	52.9
Orifice 7	55.8
Orifice 8	57.9

Thermocouple	Temperature on cooled wall, °R, for coolant flow rate, lb/sec, of -							
	0.0535	0.0500	0.0410	0.0334	0.0299	0.0250	0.0188	0.0126
1	736	850	985	1,110	1,320	1,280	1,280	1,320
2	880	761	691	825	1,295	1,175	1,250	1,295
3	---	---	---	---	---	---	---	---
4	666	681	692	732	755	770	1,202	1,278
5	600	660	676	687	720	726	938	1,250
6	650	656	656	663	683	679	722	878
7	659	668	665	668	668	673	685	732
8	---	---	---	---	---	---	---	---
9	638	---	648	---	661	---	---	661
10	---	---	---	---	---	---	---	---
11	562	571	567	571	575	571	576	580
12	632	645	644	655	655	660	661	655
13	642	658	653	658	653	664	658	653
14	695	704	695	704	704	704	704	704
15	665	669	665	669	665	665	668	703
16	660	666	660	666	667	666	670	742
17	---	---	---	---	---	---	---	---
18	667	688	683	722	716	722	1,230	1,210
19	687	736	705	763	960	753	1,200	1,260
20	---	---	---	---	---	---	---	---
21	686	---	725	---	1,195	---	---	---
22	656	679	724	679	701	---	---	1,305
23	---	---	---	---	---	---	---	---
24	665	669	726	669	666	669	675	668
25	656	668	724	668	667	668	672	667
26	656	668	724	672	667	672	679	679
27	665	673	728	673	668	674	685	673
28	666	674	729	674	669	680	690	711
29	---	---	---	---	---	---	---	---
30	666	672	726	672	720	1,315	1,315	720

TABLE I.- BASIC DATA - Continued

(d) Test B-1809

Coolant nozzle	
Type	Umbrella
Clearance, in.	0.0025
Temperature of coolant, °R	515
Total temperature of free stream, °R	2,000
Static pressure of free stream, lb/sq in. abs	14.80
Total pressure of free stream, lb/sq in. abs	120.0
α , deg	0
Model surface pressure, lb/sq in. abs, at -	
Orifice 1	55.1
Orifice 2	51.0
Orifice 3	41.5
Orifice 4	38.8
Orifice 5	54.3
Orifice 6	53.7
Orifice 7	54.5
Orifice 8	56.6

Thermocouple	Temperature on cooled wall, °R, for coolant flow rate, lb/sec, of -							
	0.1110	0.1048	0.1006	0.0945	0.0924	0.0750	0.0702	0.0535
1	835	835	711	790	1,422	1,422	1,520	1,660
2	772	747	703	713	628	628	1,425	1,585
3	---	---	---	---	---	---	---	---
4	710	705	688	694	710	722	705	920
5	708	700	688	688	700	682	694	710
6	---	---	679	679	---	---	---	---
7	702	702	686	686	707	696	690	696
8	---	---	---	---	---	---	---	---
9	---	---	---	---	---	---	---	---
10	---	---	---	---	---	---	---	---
11	571	571	567	567	571	577	571	577
12	650	662	645	650	667	678	667	682
13	686	690	675	675	690	696	686	690
14	702	702	694	689	702	702	689	696
15	710	710	699	699	710	710	699	699
16	708	713	696	696	708	708	696	703
17	---	---	---	---	---	---	---	---
18	718	723	702	702	718	723	707	723
19	732	722	684	701	722	726	910	1,162
20	---	---	---	---	---	---	---	---
21	---	---	---	---	---	---	---	---
22	702	702	680	680	708	708	690	1,580
23	---	---	---	---	---	---	---	---
24	690	690	675	680	701	696	686	690
25	672	672	665	672	688	688	679	688
26	689	695	673	674	695	701	680	689
27	697	697	665	675	697	702	686	697
28	762	754	733	733	762	762	749	754
29	---	---	---	---	---	---	---	---
30	710	710	688	688	710	710	716	750

TABLE I.- BASIC DATA - Continued

(e) Test B-1810

Coolant nozzle	
Type	Axial
Diameter, in.	0.150
Temperature of coolant, °R	510
Total temperature of free stream, °R	1,440
Static pressure of free stream, lb/sq in. abs	14.67
Total pressure of free stream, lb/sq in. abs	120.4
α , deg	0
Model surface pressure, lb/sq in. abs, at -	
Orifice 1	55.7
Orifice 2	51.7
Orifice 3	53.4
Orifice 4	50.7
Orifice 5	---
Orifice 6	57.6
Orifice 7	55.7
Orifice 8	60.9

Thermocouple	Temperature on cooled wall, °R, for coolant flow rate, lb/sec, of -							
	0.0694	0.0645	0.0597	0.0506	0.0431	0.0416	0.0299	0.0183
1	680	695	690	768	756	805	1,200	1,170
2	667	681	669	724	724	768	1,150	1,132
3	---	---	---	---	---	---	---	---
4	667	670	667	678	670	678	728	800
5	667	678	667	678	670	678	688	765
6	651	---	---	---	663	---	---	840
7	653	665	---	665	660	665	668	668
8	---	---	---	---	---	---	---	---
9	---	---	---	---	---	---	---	---
10	---	---	---	---	---	---	---	---
11	558	571	558	571	567	571	582	588
12	617	640	625	645	640	660	667	667
13	643	663	647	663	656	667	677	670
14	656	663	656	668	656	668	672	668
15	665	669	666	678	666	677	677	681
16	668	672	668	672	668	672	679	720
17	---	---	---	---	---	---	---	---
18	660	673	668	673	674	680	740	812
19	665	679	668	695	710	732	---	---
20	---	---	---	---	---	---	---	---
21	---	---	---	---	---	---	---	---
22	651	668	651	668	657	673	673	668
23	---	---	---	---	---	---	---	---
24	655	666	661	669	666	675	675	686
25	657	672	657	672	665	678	683	704
26	653	679	647	684	683	716	738	885
27	654	675	654	669	660	669	686	750
28	650	667	656	667	656	667	681	693
29	---	---	---	---	---	---	---	---
30	665	665	665	660	668	668	675	675

TABLE I.- BASIC DATA - Continued

(f) Test B-1811

Coolant nozzle

Type	Axial
Diameter, in.	0.150
Temperature of coolant, °R	510
Total temperature of free stream, °R	2,000
Static pressure of free stream, lb/sq in. abs	14.70
Total pressure of free stream, lb/sq in. abs	120.0
α , deg	0
Model surface pressure, lb/sq in. abs, at -	
Orifice 1	56.9
Orifice 2	50.2
Orifice 3	51.7
Orifice 4	49.0
Orifice 5	---
Orifice 6	57.4
Orifice 7	54.5
Orifice 8	59.3

Thermocouple	Temperature on cooled wall, °R, for coolant flow rate, lb/sec, of -							
	0.1450	0.1332	0.1221	0.1142	0.1130	0.1012	0.0924	0.0666
1	702	723	756	745	1,154	1,130	863	1,565
2	697	703	746	724	735	741	1,139	1,350
3	---	---	---	---	---	---	---	---
4	688	694	710	694	705	710	700	705
5	688	694	705	694	705	705	700	700
6	679	684	689	684	689	689	689	684
7	680	685	696	690	696	690	690	696
8	---	---	---	---	---	---	---	---
9	---	---	---	---	---	---	---	---
10	---	---	---	---	---	---	---	---
11	567	571	587	588	583	583	592	693
12	656	656	705	657	705	671	678	688
13	696	696	702	696	703	702	711	718
14	696	696	696	696	703	702	708	708
15	704	704	710	704	715	710	715	715
16	702	702	702	702	708	702	709	708
17	---	---	---	---	---	---	---	---
18	707	711	718	711	718	711	718	723
19	695	701	710	710	717	717	971	1,193
20	---	---	---	---	---	---	---	---
21	---	---	---	---	---	---	---	---
22	679	685	697	685	697	697	690	690
23	---	---	---	---	---	---	---	---
24	685	685	690	685	696	690	696	696
25	683	683	693	683	693	693	694	693
26	679	679	701	679	695	695	694	726
27	680	680	697	680	691	691	691	691
28	677	681	691	681	691	691	686	691
29	---	---	---	---	---	---	---	---
30	697	697	697	697	697	686	697	686

TABLE I.- BASIC DATA - Continued

(g) Test B-1813

Coolant nozzle	
Type	Axial
Diameter, in.	0.150
Temperature of coolant, °R	510
Total temperature of free stream, °R	2,500
Static pressure of free stream, lb/sq in. abs	14.53
Total pressure of free stream, lb/sq in. abs	119.2
α , deg	0
Model surface pressure, lb/sq in. abs, at -	
Orifice 1	----
Orifice 2	----
Orifice 3	50.2
Orifice 4	47.7
Orifice 5	----
Orifice 6	----
Orifice 7	52.1
Orifice 8	----

Thermocouple	Temperature on cooled wall, °R, for coolant flow rate, lb/sec, of -							
	0.1578	0.1487	0.1418	0.1320	0.1140	0.1118	0.0959	0.0771
1	825	726	862	799	973	---	1,568	1,740
2	781	684	807	754	798	880	935	1,540
3	---	---	---	---	---	---	---	---
4	731	680	725	680	680	725	720	788
5	736	698	742	709	709	725	709	725
6	---	---	---	---	---	---	---	---
7	714	693	714	688	671	714	704	709
8	---	---	---	---	---	---	---	---
9	---	---	---	---	---	---	---	---
10	---	---	---	---	---	---	---	---
11	577	569	577	---	569	574	569	578
12	653	653	665	659	669	669	674	690
13	687	678	697	687	691	697	697	707
14	699	684	710	699	699	709	699	710
15	712	708	723	708	708	712	708	712
16	712	701	712	701	706	712	706	712
17	---	---	---	---	---	---	---	---
18	721	705	731	709	691	712	715	709
19	---	709	---	724	751	---	794	---
20	---	---	---	---	---	---	---	---
21	---	---	---	---	---	---	---	---
22	711	694	740	701	707	720	711	718
23	---	---	---	---	---	---	---	---
24	698	692	703	698	698	703	709	709
25	701	695	701	701	701	705	705	711
26	---	---	---	---	---	---	---	---
27	---	---	---	---	---	---	---	---
28	709	694	714	694	699	709	704	709
29	---	---	---	---	---	---	---	---
30	627	616	623	616	610	616	602	688

TABLE I.- BASIC DATA - Continued

(h) Test B-1814

Coolant nozzle

Type	Axial
Diameter, in.	0.150
Temperature of coolant, °R	510
Total temperature of free stream, °R	1,440
Static pressure of free stream, lb/sq in. abs	14.55
Total pressure of free stream, lb/sq in. abs	120.4
α , deg	5
Model surface pressure, lb/sq in. abs, at -	
Orifice 1	----
Orifice 2	----
Orifice 3	58.3
Orifice 4	42.5
Orifice 5	----
Orifice 6	----
Orifice 7	52.9
Orifice 8	----

Thermocouple	Temperature on cooled wall, °R, for coolant flow rate, lb/sec, of -						
	0.0771	0.0652	0.0592	0.0571	0.0520	0.0488	0.0387
1	----	----	----	----	----	----	----
2	1,510	1,031	1,510	1,170	1,425	1,290	1,435
3	----	----	----	----	----	----	----
4	1,425	792	1,450	1,096	1,410	1,260	1,445
5	----	724	----	914	----	----	----
6	----	----	----	----	----	----	----
7	709	667	778	709	800	866	1,345
8	----	----	----	----	----	----	----
9	----	----	----	----	----	----	----
10	----	----	----	----	----	----	----
11	568	552	573	559	573	569	589
12	673	642	684	658	679	673	722
13	691	653	691	664	681	671	873
14	695	660	695	679	688	701	1,179
15	701	667	734	689	817	811	1,315
16	717	681	891	759	1,215	1,044	1,350
17	----	----	----	----	----	----	----
18	1,405	780	1,400	1,047	1,280	1,229	1,405
19	----	891	----	1,082	----	----	----
20	----	990	----	1,125	----	----	----
21	----	----	----	----	----	----	----
22	682	643	687	654	677	666	681
23	----	----	----	----	----	----	----
24	712	681	875	775	1,255	1,108	1,398
25	769	709	1,270	805	1,360	1,202	1,440
26	----	----	----	----	----	----	----
27	----	----	----	----	----	----	----
28	834	743	1,378	865	1,385	1,220	1,432
29	----	----	----	----	----	----	----
30	862	643	693	660	681	670	681

TABLE I.- BASIC DATA - Continued

(i) Test B-1815

Coolant nozzle

Type	Umbrella
Clearance, in.	0.0025
Temperature of coolant, °R	510
Total temperature of free stream, °R	1,440
Static pressure of free stream, lb/sq in. abs	14.57
Total pressure of free stream, lb/sq in. abs	120.4
α , deg	5
Model surface pressure, lb/sq in. abs, at -	
Orifice 1	----
Orifice 2	----
Orifice 3	48.8
Orifice 4	35.1
Orifice 5	----
Orifice 6	----
Orifice 7	50.0
Orifice 8	----

Thermocouple	Temperature on cooled wall, °R, for coolant flow rate, lb/sec, of -							
	0.0840	0.0735	0.0722	0.0596	0.0500	0.0416	0.0250	0.0167
1	----	----	----	----	----	----	----	----
2	829	1,270	1,083	1,305	1,305	1,287	1,310	1,313
3	----	----	----	----	----	----	----	----
4	735	712	935	768	768	768	768	746
5	----	----	----	----	----	----	----	----
6	----	----	----	----	----	----	----	----
7	650	970	651	862	----	1,288	1,318	1,318
8	----	----	----	----	----	----	----	----
9	----	----	----	----	----	----	----	----
10	----	----	----	----	----	----	----	----
11	533	538	538	553	568	595	660	735
12	615	626	630	652	717	1,044	1,197	1,238
13	643	658	647	663	916	1,163	1,249	1,279
14	653	666	653	670	1,285	1,285	1,305	1,305
15	656	684	656	745	1,320	1,320	1,320	1,333
16	652	710	670	804	1,318	1,318	1,318	1,323
17	----	----	----	----	----	----	----	----
18	703	1,196	768	1,080	1,313	1,313	1,313	1,319
19	----	----	----	----	----	----	----	----
20	769	1,223	1,029	1,083	1,275	1,274	1,295	1,311
21	----	----	----	----	----	----	----	----
22	615	621	626	643	660	666	681	631
23	----	----	----	----	----	----	----	----
24	663	723	687	1,153	1,318	1,318	1,335	1,345
25	671	866	744	1,325	1,330	1,325	1,345	1,350
26	----	----	----	----	----	----	----	----
27	----	----	----	----	----	----	----	----
28	671	1,247	774	1,320	1,320	1,320	1,332	1,320
29	----	----	----	----	----	----	----	----
30	586	597	711	578	578	637	827	898

TABLE I.- BASIC DATA - Continued

(j) Test B-1816

Coolant nozzle

Type	Axial
Diameter, in.	0.050
Temperature of coolant, °R	None
Total temperature of free stream, °R	1,360
Static pressure of free stream, lb/sq in. abs	14.80
Total pressure of free stream, lb/sq in. abs	120.5
α , deg	0
Model surface pressure, lb/sq in. abs, at -	
Orifice 1	----
Orifice 2	----
Orifice 3	53.5
Orifice 4	51.3
Orifice 5	----
Orifice 6	----
Orifice 7	55.8
Orifice 8	----

[illegible]

TABLE I.- BASIC DATA - Concluded

(k) Test B-1818

Coolant nozzle	
Type	Axial
Diameter, in.	0.150
Temperature of coolant, °R	510
Total temperature of free stream, °R	3,060
Static pressure of free stream, lb/sq in. abs	14.90
Total pressure of free stream, lb/sq in. abs	118.7
α , deg	0
Model surface pressure, lb/sq in. abs, at -	
Orifice 1	----
Orifice 2	----
Orifice 3	50.3
Orifice 4	48.6
Orifice 5	----
Orifice 6	----
Orifice 7	54.6
Orifice 8	----

Thermocouple	Temperature on cooled wall, °R, for coolant flow rate, lb/sec, of -							
	0.2140	0.1970	0.1913	0.1844	0.1790	0.1705	0.1614	0.1490
1	---	---	---	---	---	---	---	---
2	723	735	830	830	790	830	832	880
3	---	---	---	---	---	---	---	---
4	710	720	733	738	721	738	718	738
5	---	---	---	---	---	---	---	---
6	---	---	---	---	---	---	---	---
7	695	706	733	727	710	727	719	733
8	---	---	---	---	---	---	---	---
9	---	---	---	---	---	---	---	---
10	---	---	---	---	---	---	---	---
11	570	570	610	599	567	586	576	576
12	650	661	670	670	655	678	678	682
13	681	687	702	702	697	706	707	710
14	900	705	716	710	711	717	717	722
15	713	713	725	713	720	720	725	731
16	712	719	724	719	719	719	724	730
17	---	---	---	---	---	---	---	---
18	711	718	734	728	722	728	728	734
19	---	---	---	---	---	---	---	---
20	717	749	---	---	780	---	---	---
21	---	---	---	---	---	---	---	---
22	---	---	---	---	---	---	---	---
23	---	---	---	---	---	---	---	---
24	694	704	713	720	713	720	720	720
25	694	704	720	710	705	720	710	713
26	---	---	---	---	---	---	---	---
27	---	---	---	---	---	---	---	---
28	678	703	728	728	712	723	723	728
29	---	---	---	---	---	---	---	---
30	624	531	536	531	531	616	531	531

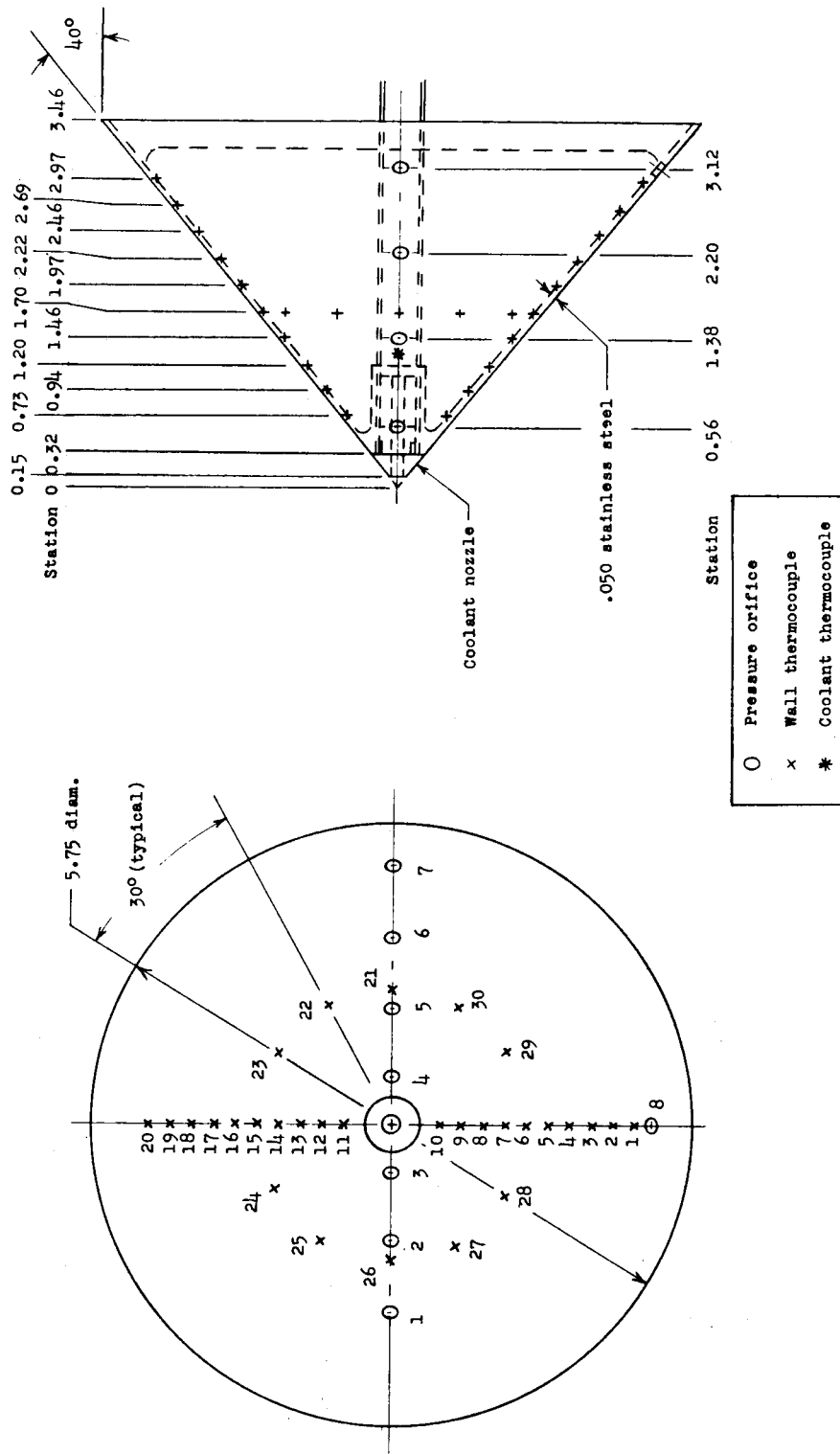
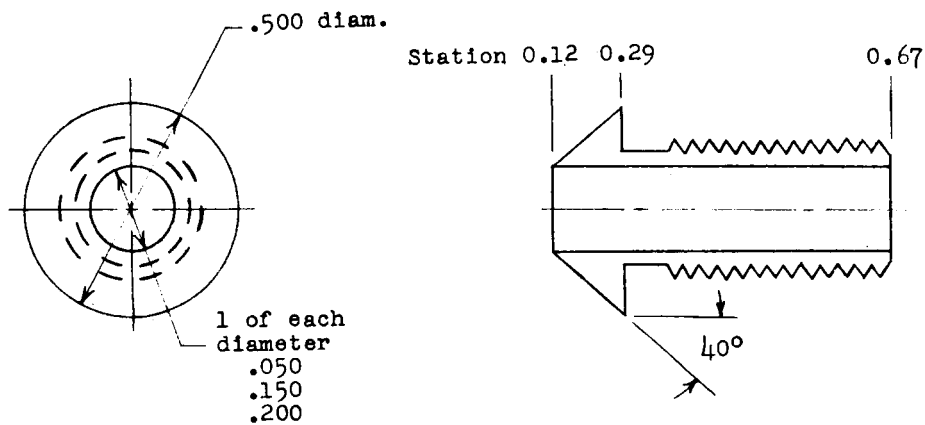
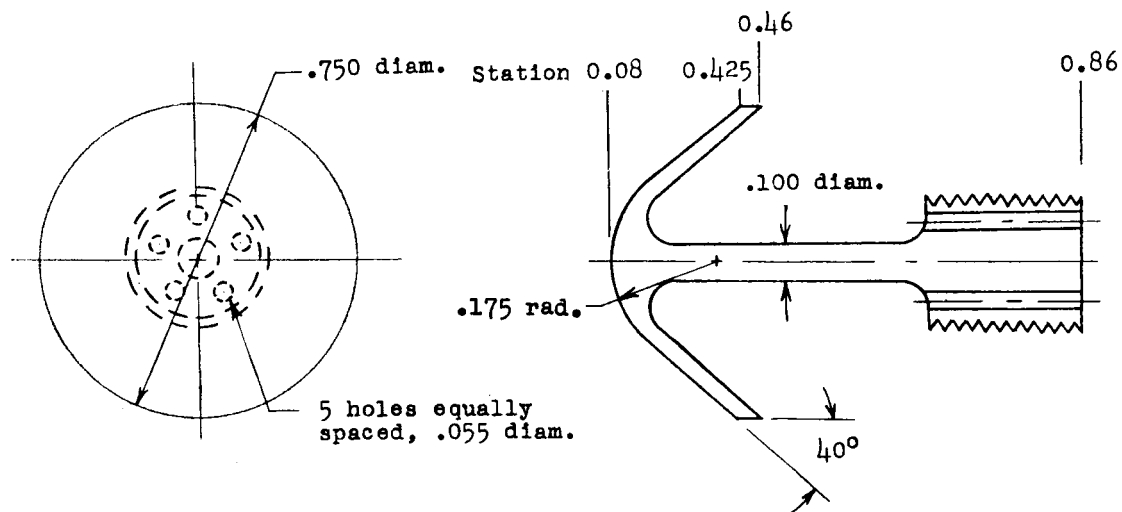


Figure 1.- Drawing of 80° total-angle cone showing locations of thermocouples and pressure orifices. All dimensions are in inches.

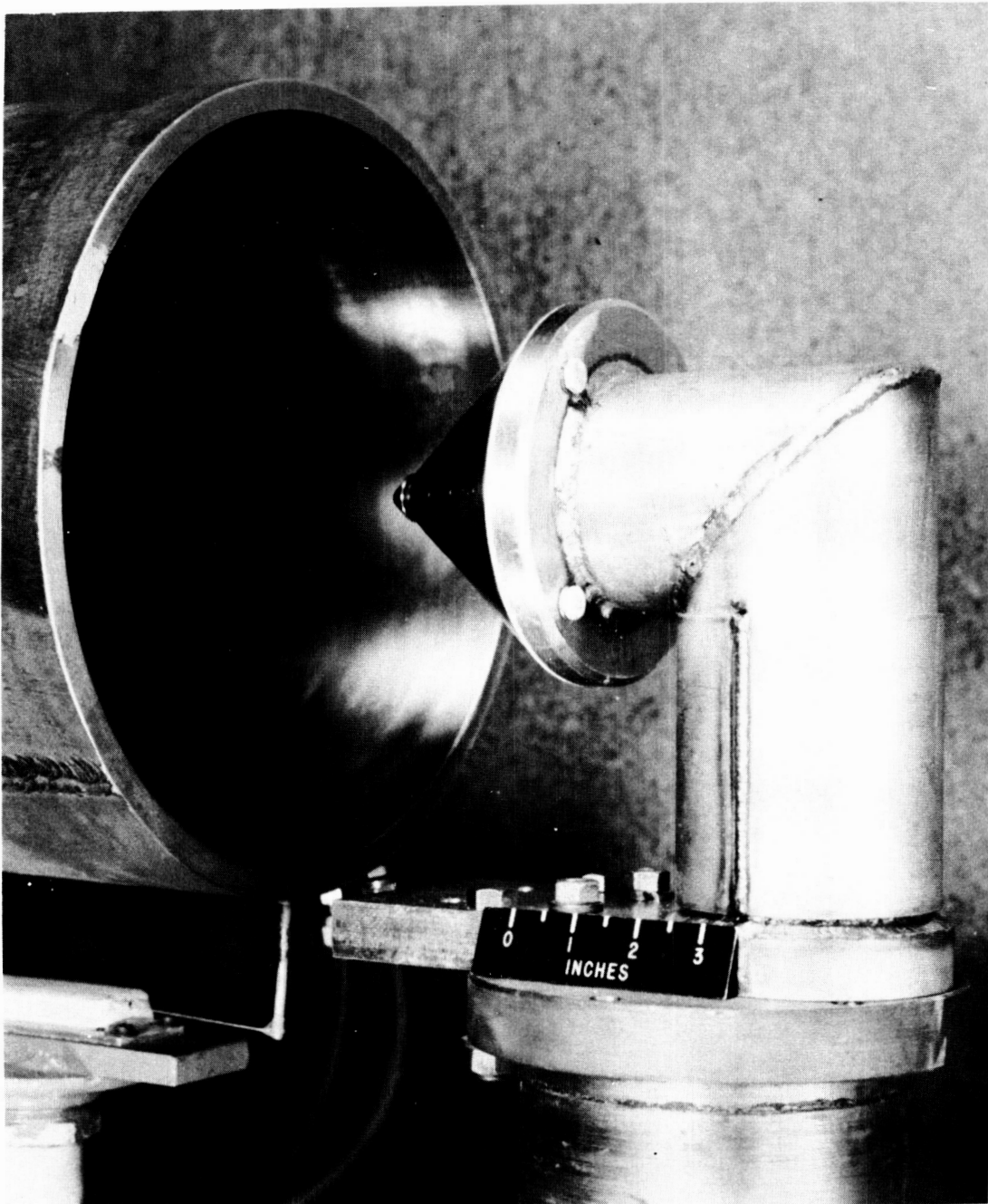


Axial nozzles



Umbrella nozzle

Figure 2.- Drawings of the four nozzles (not to scale). All dimensions are in inches.



L-57-5198

Figure 3.- Photograph of the 80° total-angle cone mounted in the ethylene-heated high-temperature jet.

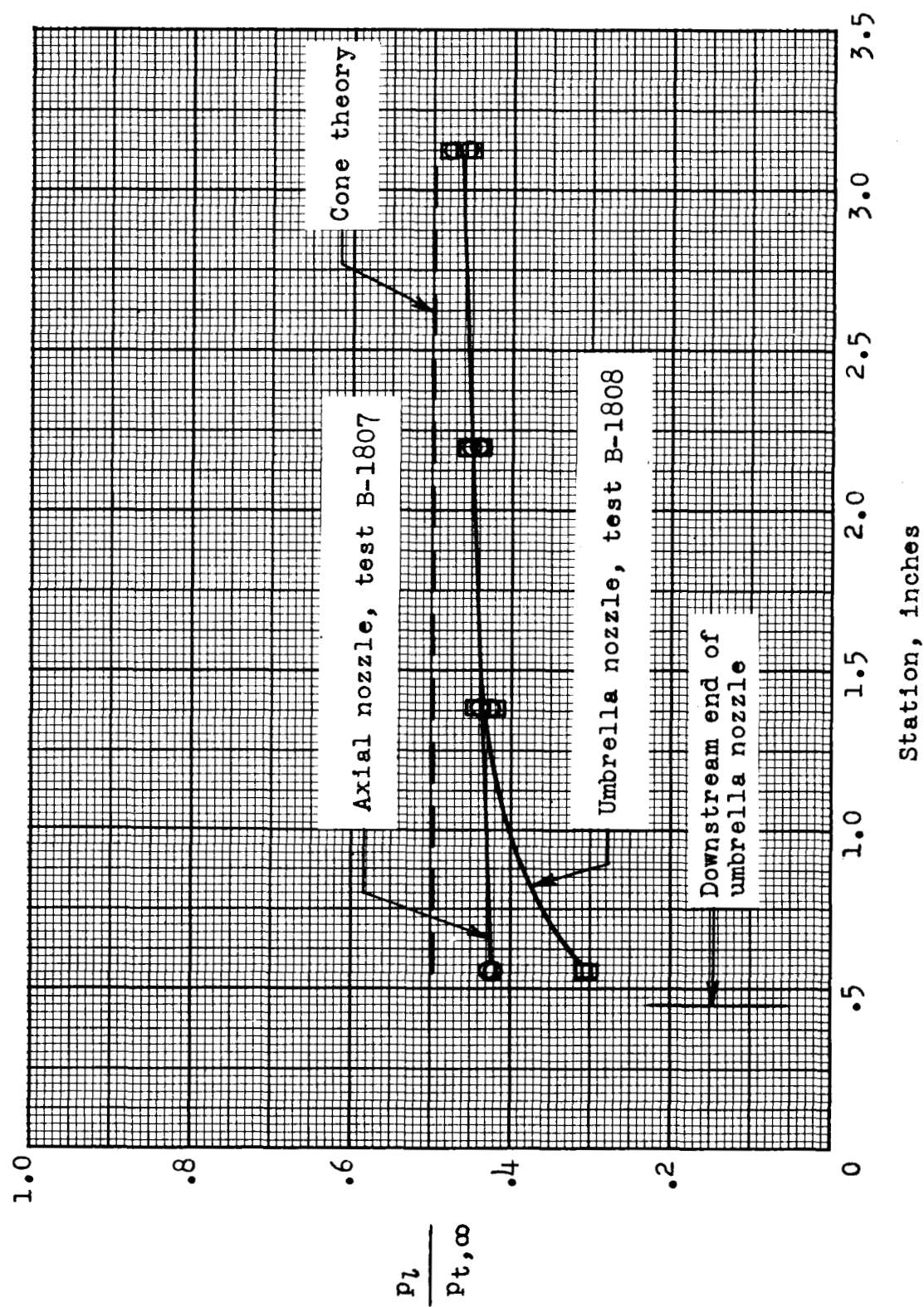


Figure 4.- Typical pressure distributions for the two types of coolant flow nozzles.

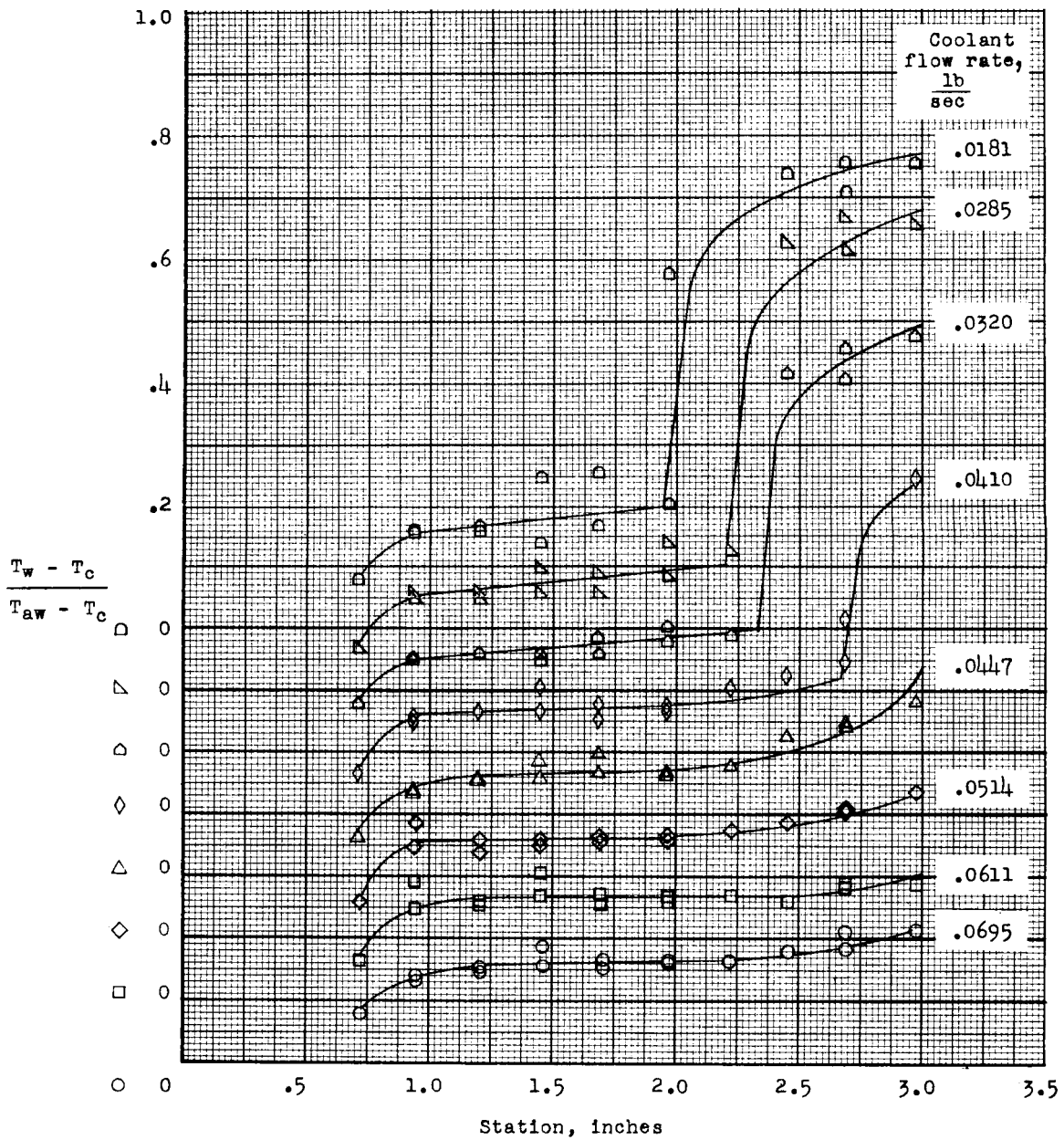


Figure 5.- Temperature distributions for a series of coolant flow rates from a typical test (test B-1807).

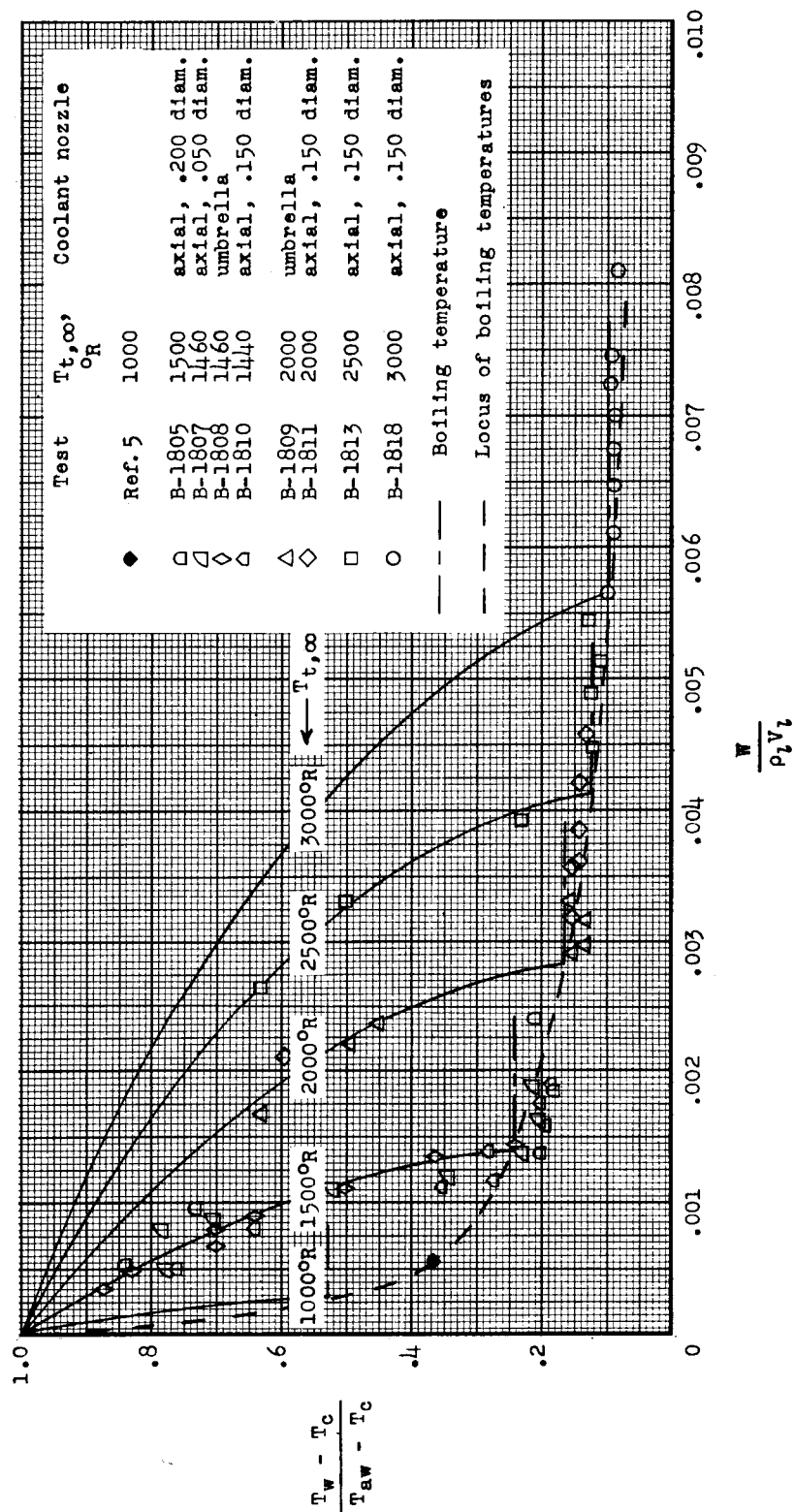


Figure 6.- Effect of flow rate parameter on the temperatures at the thermocouple station farthest downstream.

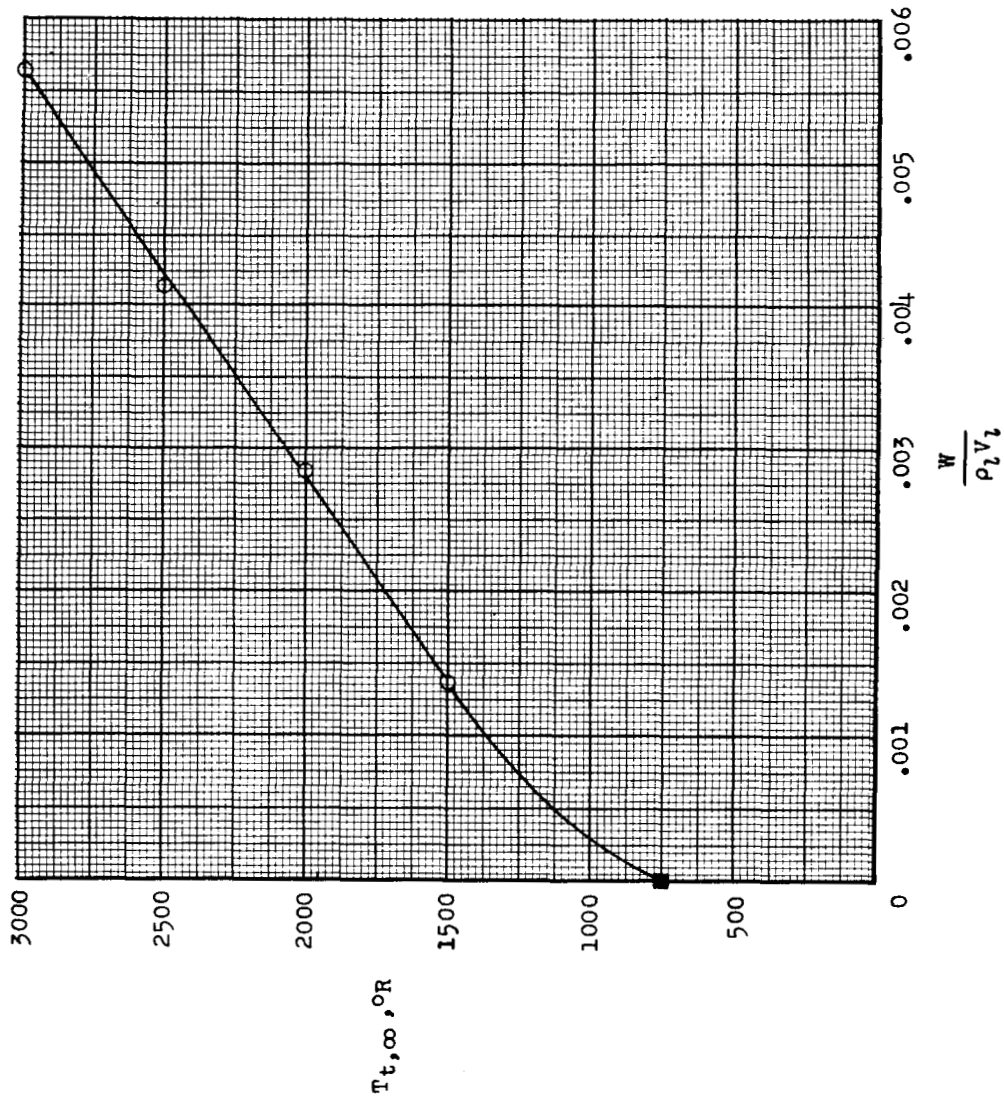


Figure 7.- Minimum flow rates necessary to maintain boiling temperature of coolant (approximately 750° R for this model) at thermocouple station farthest downstream as a function of free-stream total temperature.

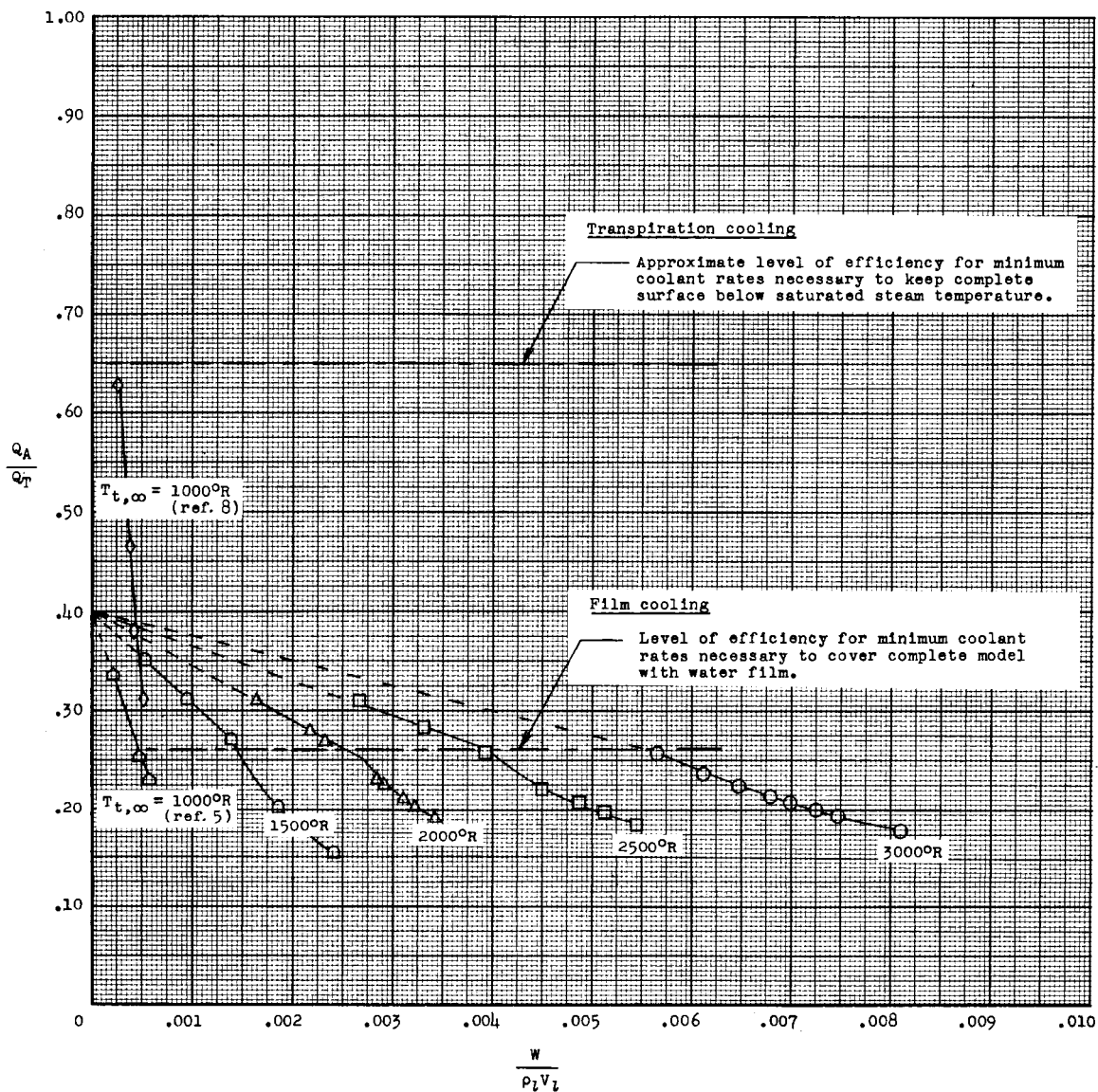


Figure 8.- Efficiency of film cooling from reference 5 and present tests, and of transpiration cooling from reference 8.

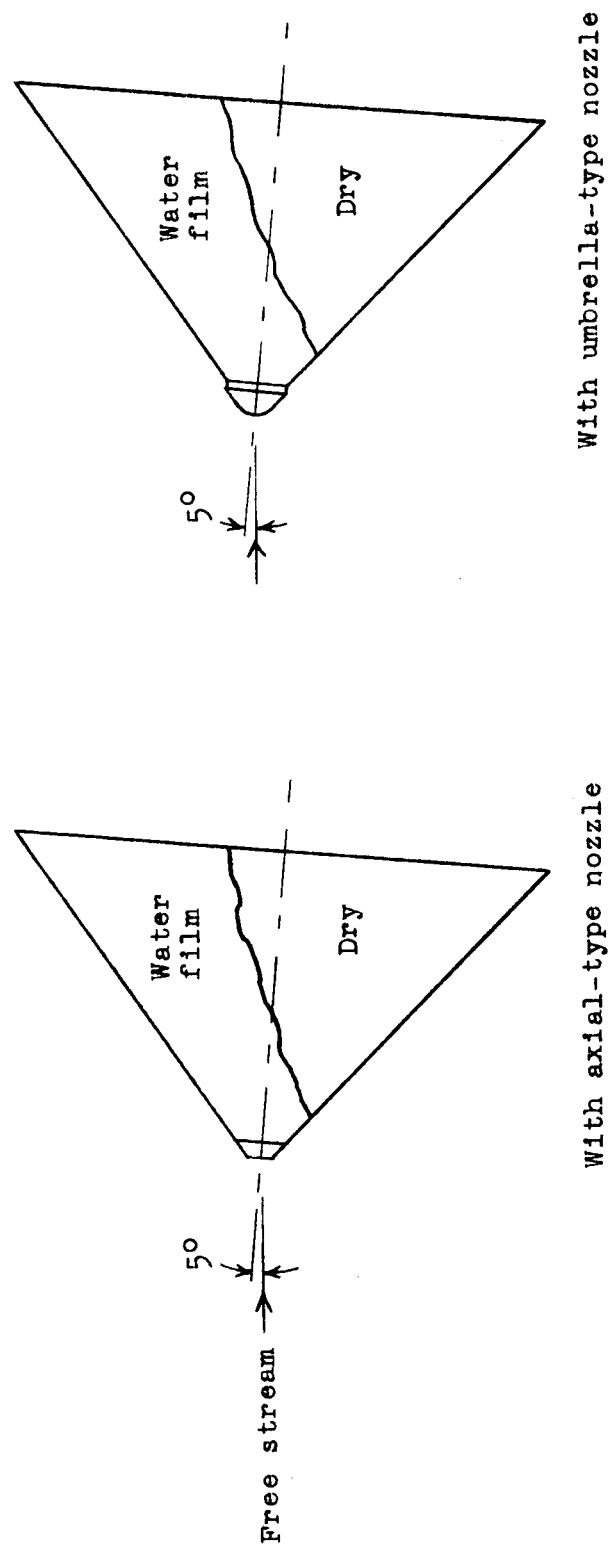


Figure 9.- Sketch showing approximately the water film asymmetry at $\alpha = 5^\circ$ for each type of coolant nozzle.